

Variational Approach of Constructing Reduced Fluid-Structure Interaction Models in Bifurcated Networks

A. S. Liberson, Y. Seyed Vahedein, D. A. Borkholder

Rochester Institute of Technology

James E. Gleason Building, 76 Lomb Memorial Drive, Rochester, NY 14623-5604, United States

asleme@rit.edu; yashar.seyed.vahedein@rit.edu; david.borkholder@rit.edu

Abstract - Reduced fluid-structure interaction models have received a considerable attention in recent years being the key component of hemodynamic modeling. A variety of models applying to specific physiological components such as arterial, venous and cerebrospinal fluid (CSF) circulatory systems have been developed based on different approaches. The purpose of this paper is to apply the general approach based on Hamilton's variational principle to create a model for a viscous Newtonian fluid - structure interaction (FSI) in a compliant bifurcated network. This approach provides the background for a correct formulation of reduced FSI models with an account for arbitrary nonlinear visco-elastic properties of compliant boundaries. The correct boundary conditions are specified at junctions, including matching points in a combined 3D/1D approach. The hyperbolic properties of derived mathematical model are analyzed and used, constructing the monotone finite volume numerical scheme, second-order accuracy in time and space. The computational algorithm is validated by comparison of numerical solutions with the exact manufactured solutions for an isolated compliant segment and a bifurcated structure. The accuracy of applied TVD (total variation diminishing) and Lax-Wendroff methods are analyzed by comparison of numerical results to the available analytical smooth and discontinuous solutions.

Keywords: Hamilton's variational principle, reduced fluid-structure interaction (FSI), bifurcated arterial networks, multiscale 3D/1D approach, total variation diminishing method (TVD), Lax-Wendroff method, manufactured test, break-down solution

Nomenclature

PWV: Pulse wave velocity (m/s)

FSI : Fluid structure interaction

A : Cross sectional area (m²)

V : Velocity Vector(m/s)

u : Displacement vector (m)

p : pressure (Pa)

ρ : Density of incompressible fluid (kg/m³)

U : Internal Energy (J)

R, r : Internal wall radii in a zero stress and loaded conditions respectively (m)

η : Ratio of the wall deflection to R

c : Moens–Korteweg speed of Propagation (m/s)

σ, τ : Axial normal and shear viscous stress (Pa)

ν : Kinematic viscosity (m²/s)

1. Introduction

An extensive work has been done for developing different models, applied to specific components of hemodynamic pulsating flow, such as arterial, venous and CSF circulations. A historical review of arterial fluid mechanics models was presented by Parker – 2009 [1]. Detailed derivation of simplified reduced FSI models for a linear elastic arterial system with account of visco-elasticity and inertia of the wall can be found in Formaggia et al. – 2009 [2]. Physical nonlinearity of thin and thick walls coupled with large deformations have been introduced in FSI dynamics by Liberson et al. – 2016 [3] and Lillie et al. – 2016 [4]. An analytical solution for the pulse wave velocity (PWV) of a nonlinear FSI model was

presented in Liberson et al. – 2014 [5]. The variational approach, yielding governing equations of physical phenomena, serves as an indispensable tool in case, when the interaction of the system components are non-trivial, containing, as an example, strong nonlinearities, kinematic constraints, high derivatives. The monumental book of Berdichevsky – 2010 [6] presents a variety of variational principles applied separately to fluids and solids. Kock and Olson - 1991 [7] developed a variational approach for FSI system, restricting analysis by a linear elastic thin-walled cylinder and an inviscid, irrotational and isentropic fluid flow. Lagrangian multipliers are used to reinforce continuity equation and boundary conditions. Multiple references can be found in this paper relating to applications of the variational approach to the analysis of small vibrations of elastic bodies in a potential fluid.

We demonstrate the effectiveness of Hamiltonian variational principle in analyzing FSI without any limitations on dissipative fluid dynamics and physical properties of an adjacent flow path wall. We do not use the Lagrangian multiplier, accounting for the continuity equation explicitly, which simplifies the entire procedure. Internal boundary conditions are specified at junctions, including matching points in a combined 3D/1D approach, following from the Euler-Lagrange conditions.

Numerical effectiveness in a simulation of a pulsating flow is characterized by its ability to track a propagating wave for a few periods without suffering from numerical dissipation (errors in amplitude) and numerical dispersion (artificial oscillations). The most popular numerical methods in this area are the Lax-Wendroff finite volume method, its Taylor-Galerkin finite element counterpart, and a discontinuous Galerkin spectral finite element method [2]. We demonstrate superiority in accuracy, for the second order approximation, TVD method [8-10], which could be essential when simulating a model with discontinuity in the load or material properties

2. The Variational Principle for Fluid–Structure Interaction Problems

Hamilton’s variational principle is enunciated as a universal principle of nature unifying mechanical, thermodynamic, electromagnetic and other fields in a single least action functional, subject to extremization for a true process. According to the mentioned principle, the variation of the action functional δI being applied to FSI problem can be determined as:

$$\delta I = \delta I_{fluid} + \delta I_{solid} = \int_{t1}^{t2} \left[\oint_{\forall_{fluid}(t)} \rho_f \delta L_f d\forall + \oint_{\forall_{solid}(t)} \delta L d\forall \right] dt = 0 \quad (1)$$

Here $\delta I_{fluid}, \delta I_{solid}$ are variations of action components across fluid and solid volumes $\forall_{fluid}(t), \forall_{solid}(t)$; t – time, ρ_f -density of the fluid, L_f, L - the Lagrangian density functions for fluid and solids respectfully.

2.1. Fluid Domain

As it is mentioned by Berdichevsky - 2010 [6], variation of the Lagrange function density in Eulerian coordinates can be written as follows:

$$\delta L_f = \delta \left(\frac{\mathbf{V}^2}{2} - U(\rho_f, S, \nabla \mathbf{u}) \right) + T \delta S \quad (2)$$

Where \mathbf{V} – is a velocity vector, U – is an internal energy as a function of density, entropy S , and a distortion tensor $\nabla \mathbf{u}$ (gradient of a displacement vector \mathbf{u}), T – temperature. Velocity, density and the displacement vector are not subject to independent variations. To avoid the use of Lagrangian multipliers extract variation of density directly from the mass conservation law:

$$\delta(\rho_f d\forall) = 0 \rightarrow \delta \rho_f = -\rho_f \nabla \cdot \mathbf{u} \quad (3)$$

Presenting variation of a velocity as a substantial derivative of a variation of a displacement vector, arrive at:

$$\delta \mathbf{V} = \frac{D\delta \mathbf{u}}{Dt} = \frac{\partial \delta \mathbf{u}}{\partial t} + \mathbf{V} \cdot \nabla \delta \mathbf{u} \quad (4)$$

Now we have reduced the equation (2) to the only independent variables - displacement and entropy. Substituting (3) and (4) into equation (2) gives:

$$\delta I_{fluid} = \int_{t_1}^{t_2} \left[\oint_{\mathcal{V}_{fluid}(t)} \left(\rho_f \mathbf{V} \cdot \left(\frac{\partial \delta \mathbf{u}}{\partial t} + \mathbf{V} \cdot \nabla \delta \mathbf{u} \right) + p \nabla \cdot \delta \mathbf{u} - \frac{\rho_f \partial U}{\partial \rho_f} \delta \rho_f - \rho_f \left(\frac{\partial U}{\partial s} - T \right) \delta s - \boldsymbol{\sigma} : \delta \nabla \mathbf{u} \right) d\mathcal{V} \right] dt \quad (5)$$

In which, according to Maxwell's thermodynamic identity, pressure $p = \rho_f^2 \frac{\partial U}{\partial \rho}$, and the deviatoric stress tensor is introduced as $\boldsymbol{\sigma} = \rho_f \frac{\partial U}{\partial \nabla \mathbf{u}}$.

Considering 2D axisymmetric flow in a long compliant tube, according to the long wave approximation we neglect variability of a radial velocity component and a pressure in a radial direction. The equation (5) in this case is transformed to the following form:

$$\delta I_{fluid} = \int_{t_1}^{t_2} \int_x \int_0^{R(x,t)} \left[\rho_f V \left(\frac{\partial \delta u}{\partial t} + V \frac{\partial \delta u}{\partial x} \right) + P \frac{\partial \delta u}{\partial x} - \sigma \frac{\partial \delta u}{\partial x} - \tau \frac{\partial \delta u}{\partial r} \right] r dr dx dt \quad (6)$$

Here V – is an axial velocity, u – is an axial component of displacement, σ, τ – axial normal and shear viscous stress components, $R(x, t)$ - internal radius of a tube as a function of axial coordinate and time. The reduced models are based on assumptions regarding radial profiles, i.e.

$$V(x, r, t) = \varphi(r) \bar{V}(x, t); \quad u(x, r, t) = f(r) \bar{u}(x, t) \quad (7)$$

With the aim of application to the incompressible flow, density is assumed constant. Integrating the functional (7) over the cross section with the following integration by parts, arrive at the reduced momentum equation

$$\frac{\partial \bar{V}}{\partial t} + \frac{\partial}{\partial x} \left(a_1 \frac{p}{\rho} + a_2 \bar{V}^2 \right) = \frac{1}{a_0 \rho} \left[\int r f(r) \sigma(x, r, t) dr - R \tau(x, R, t) \right] \quad (8)$$

Where the coefficients are:

$$a_0 = \int r f(r) dr; \quad a_1 = \int r \varphi(r) f(r) dr; \quad a_2 = \frac{1}{a_0} \int r \varphi(r)^2 f(r) dr \quad (9)$$

In case of Newtonian fluid ($\sigma = 2\rho v \frac{\partial V}{\partial x}$, $\tau = \rho v \frac{\partial V}{\partial r}$), generalized Hagen-Poiseuille profile $\varphi(r) = \frac{\gamma+2}{\gamma} \left[1 - \left(\frac{r}{R} \right)^\gamma \right]$ and a constant profile for the function distribution in radial direction, $f(r) = 1$, equation (8) takes the form presented by San and Staples – 2012 [12].

$$\frac{\partial \bar{V}}{\partial t} + \frac{\partial}{\partial x} \left(\alpha \frac{\bar{V}^2}{2} + \frac{P}{\rho} \right) = v \left(\frac{\partial^2 \bar{V}}{\partial x^2} - 2(\gamma + 2) \frac{\bar{V}}{R^2} \right) \quad (10)$$

Besides equation (8), Hamilton's equation in a form of $\delta I_{fluid} = 0$ yields natural boundary conditions. In case of a multiscale model, matching section of a coupled 3D and 1D require continuity following from natural boundary conditions

$$a_1 \frac{p}{\rho} + a_2 \bar{V}^2 = \int r f(r) \left(\frac{p}{\rho} + V^2 \right) dr \quad (11)$$

It should be noted that we neglect the effect of dissipation on boundary conditions.

2.2. Solid Domain

Consider a circular thin-wall cylinder relating to the polar system of coordinates. Let R be the radius of the wall under the load, R_0 – radius in a load free state, h - the wall thickness, $\lambda_\theta = R/R_0$ – circumferential stretch ratio, $\eta = (\lambda_\theta - 1)$ – nondimensionalized wall normal displacement. Introducing wall kinetic energy K , elastic energy U_{el} and a dissipative energy U_d and work of external load W_p the Hamiltonian functional relating to the solid domain can be presented as

$$\delta I_{solid} = \iint (\delta K - (\delta U_{el} + \delta U_d - \delta W_p)) dx dt \quad (12)$$

Kinetic energy per unit length is defined by the normal velocity of the moving wall $R_0 \frac{d\eta}{dt}$

$$K = \frac{1}{2} \rho h R_0^2 (1 + \eta) \left(\frac{\partial \eta}{\partial t} \right)^2 \quad (13)$$

Internal elastic energy is composed of hyperelastic exponential strain energy (Fung, 1990) and an energy, accumulated by a longitudinal pre-stress force N per unit area

$$U_{el} = \frac{c}{2} (e^Q - 1) + N \left(\sqrt{1 + R_0^2 \left(\frac{\partial \eta}{\partial x} \right)^2} - 1 \right) \quad (14)$$

Where $Q = a_{11} E_\theta^2 + 2a_{12} E_\theta E_z + a_{22} E_z^2$, and $c, a_{11}, a_{12}, a_{22}$ are material constants from Fung et al. anisotropic model [11]. Assuming the wall model is a system of independent nonlinearly elastic rings, and simplifying the equation (14) by leaving the principle quadratic terms only (the forth power for η and quadratic terms for the slope), arrive at

$$U_{el} = \frac{ca_{11}}{8} (\eta^4 + 4\eta^3 + 4\eta^2) + \frac{N}{2} R_0^2 \left(\frac{\partial \eta}{\partial x} \right)^2 \quad (15)$$

Elementary work produced by the viscous component of circumferential stress relating to the Voight type of material and external pressure load are presented as

$$\delta U_d - \delta W_p = \left(\frac{\mu h}{R_0} \frac{\partial \eta}{\partial t} - p \right) R_0 \delta \eta \quad (16)$$

Substituting (13)-(16) into equation (12), and equating to zero, obtain the equation of motion of an axisymmetric cylinder in the explicit form with respect to pressure

$$p = \rho h R_0 \frac{\partial^2 \eta}{\partial t^2} + \frac{\mu h}{R_0} \frac{\partial \eta}{\partial t} + ca_{11} \left(\frac{3}{2} \eta^2 + \eta \right) - N R_0^2 \frac{\partial^2 \eta}{\partial x^2} \quad (17)$$

Momentum equation (8), equation of a boundary wall motion (17) and an averaged over the cross-section continuity equation (3)

$$\frac{\partial A}{\partial t} + \frac{\partial}{\partial x}(\bar{V}A) = 0; \quad A=(\eta + 1)^2 \quad (18)$$

Create a closed-form reduced mathematical model for fluid-structure interaction in a compliant channel.

3. Numerical Simulation

The most popular numerical methods in computational hemodynamics are the Lax-Wendroff finite volume method, its Taylor-Galerkin finite element counterpart, and a discontinuous Galerkin spectral finite element method [2]. In this paper, we apply the second-order accuracy in time and space with TVD method, which demonstrates its superiority when simulating a discontinuity in a load or in material properties. The details of TVD methods applied to the system of hyperbolic equations could be found in [8].

3.1. Break-down Solution

To compare the behavior of numerical solutions of Lax-Wendroff and TVD methods, Fig. 1 and Fig. 2 show evolution of the initial discontinuity of pressure and velocity, according to the following acoustics counterpart of equations (16)-(18)

$$\begin{aligned} \frac{\partial p}{\partial t} + \rho c^2 \frac{\partial v}{\partial x} &= 0; \\ \frac{\partial v}{\partial t} + \frac{1}{\rho} \frac{\partial p}{\partial x} &= 0; \end{aligned} \quad (19)$$

The same values of $\rho=0.25 \frac{kg}{m^3}$, $c = 2 \frac{m}{s}$, Courant number CFL=0.5 and cell count of n=100 was used for both schemes. Discontinuity is resolved perfectly by the TVD method, reproducing practically the exact solution (Fig. 1). Discontinuity give rise to artificial oscillations when Lax-Wendroff method is used. The Lax-Wendroff method is clearly dispersive, and does not perform well around discontinuities.

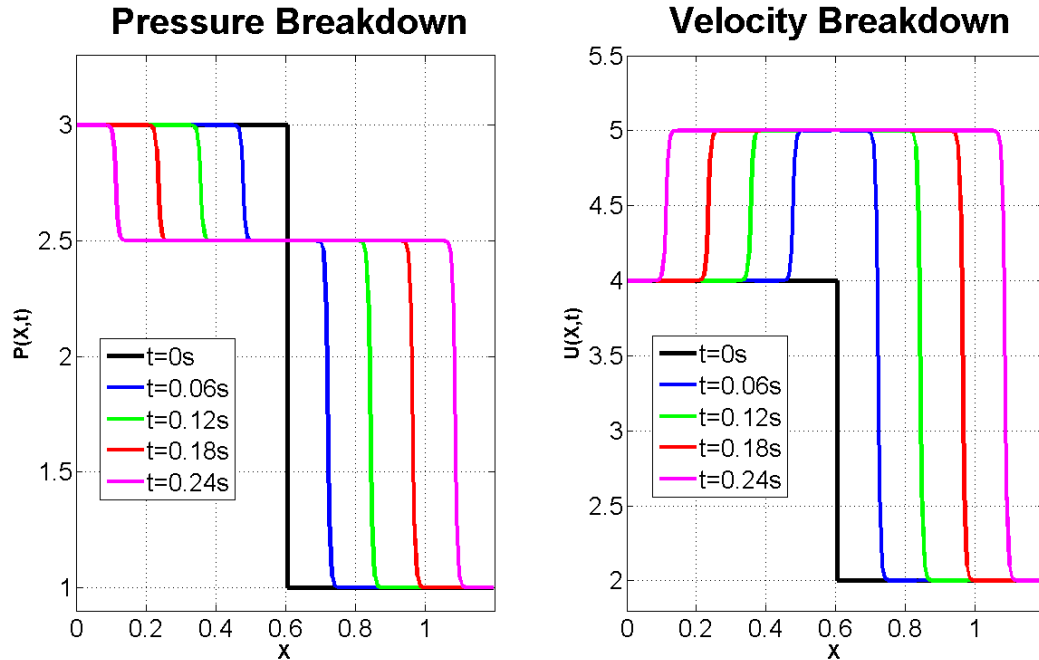


Fig. 1: TVD test. Evolution of discontinuity.

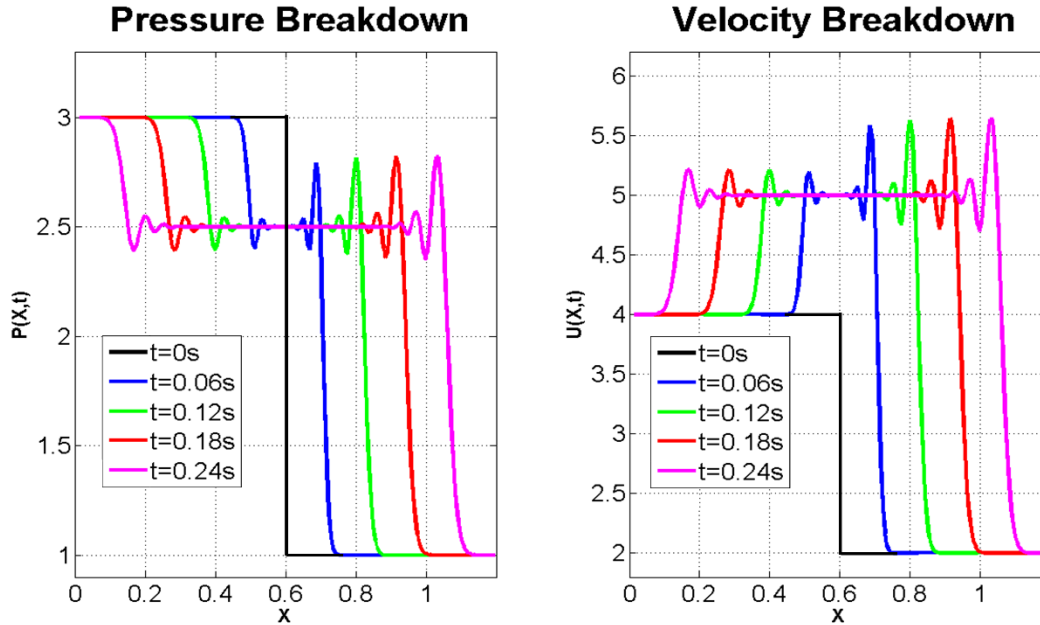


Fig. 2: Lax-Wendroff test. Evolution of discontinuity.

3.2. Single Segment Nonlinear FSI Problem Testing Case

The nonlinear mathematical model used for this problem is based on momentum equation (10) ($\alpha=1$), continuity equation (18) and a linear constituent equation in the form of (17), accounting for the linear viscoelastic behavior of the wall. We start manufacturing an explicit expression for the solution as a superposition of Fourier harmonics, satisfying the corresponding linear equations. Then, we substitute the solution to the equations (10), (17) and (18), evaluating the source terms. Given the source terms, boundary and initial conditions just obtained, we use the simulation tool to obtain a numerical solution and compare it to the originally assumed solution with which we started. Results, presented in Fig. 3 prove that plots cannot distinguish between numerical and exact solution. For smooth solutions, the Lax-Wendroff approach and TVD solutions give practically the same answer.

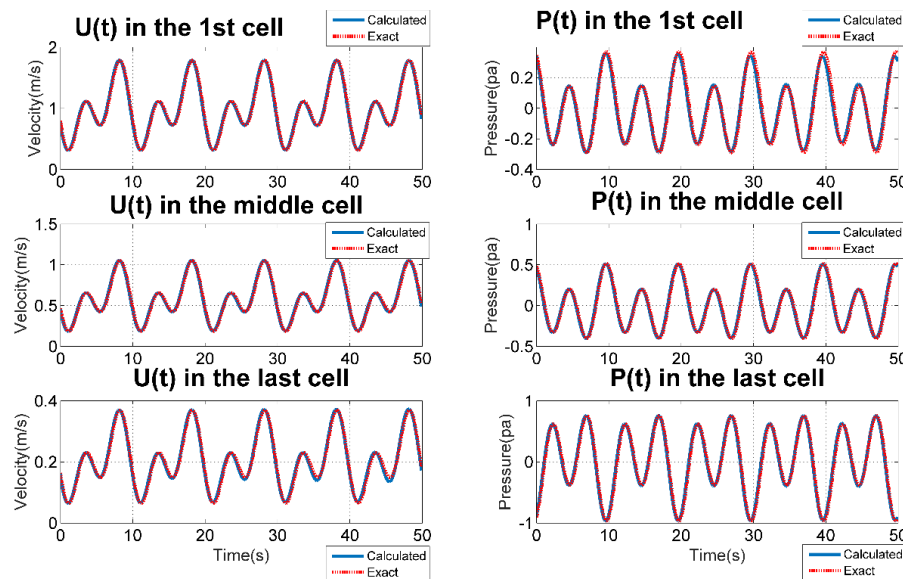


Fig. 3: FSI problem for a single segment. Velocity and pressure distributions in the center of the 1st cell,

middle cell and the last cell. Numerical and manufactured solutions are not distinguishable.

3.3. Bifurcated Elements Nonlinear FSI Problem Testing Case

Schematic of a symmetric bifurcated structure with a single parent vessel and two identical daughters (twins) is presented in Fig. 4. We have manufactured an explicit expression for the solution as a superposition of three Fourier harmonics, satisfying a priori flow and pressure continuity at the matching sections. The flow for the daughter

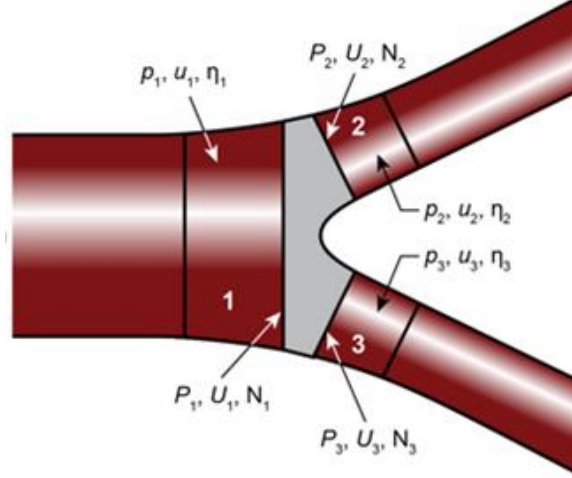


Fig. 4: Schematic of bifurcated vessels.

Q_d and parent Q_p vessels are created such that the continuity condition at matching sections is satisfied automatically, $Q_p(x = L_3, t) = 2Q_d(x = 0, t)$, and x – is the local coordinate at each vessel, varying from 0 to L_1 in daughter segment, and from 0 to L_3 in a parent vessel.

$$Q_d = q_1 \cos(2\pi t) \cos\left(2\pi \frac{x}{L_1}\right) + q_2 \cos(4\pi t) \cos\left(4\pi \frac{x}{L_1}\right) + q_3 \cos(6\pi t) \cos\left(6\pi \frac{x}{L_1}\right) \quad (20)$$

$$Q_p = 2q_1 \cos(2\pi t) \cos\left(2\pi \frac{x}{L_3}\right) + 2q_2 \cos(4\pi t) \cos\left(4\pi \frac{x}{L_3}\right) + 2q_3 \cos(6\pi t) \cos\left(6\pi \frac{x}{L_3}\right) \quad (21)$$

The pressure distributions for the parent $P_p(x, t)$ and the daughter $P_d(x, t)$ vessels are manufactured providing automatically match $P_p(x = L_3, t) = P_d(x = 0, t)$ at junctions.

$$P_d = p_1 \cos(2\pi t) \cos\left(2\pi \frac{x}{L_1}\right) + p_2 \cos(4\pi t) \cos\left(4\pi \frac{x}{L_1}\right) + p_3 \cos(6\pi t) \cos\left(6\pi \frac{x}{L_1}\right) \quad (22)$$

$$P_p = p_1 \cos(2\pi t) \left(1 + \sin\left(2\pi \frac{x}{L_3}\right)\right) + p_2 \cos(4\pi t) \left(1 + \sin\left(4\pi \frac{x}{L_3}\right)\right) + p_3 \cos(6\pi t) \left(1 + \sin\left(6\pi \frac{x}{L_3}\right)\right) \quad (23)$$

As mentioned before, we substitute the solution to the equations (10), (17) and (18), evaluating the source terms. Given the source terms, boundary and initial conditions just obtained, we use the simulation tool to obtain a numerical solution and compare it to the originally assumed solution with which we started. Results, presented in Fig. 5 prove that plots cannot distinguish between numerical and exact solution. For smooth solutions, the Lax-Wendroff approach and TVD solutions give practically the same answer.

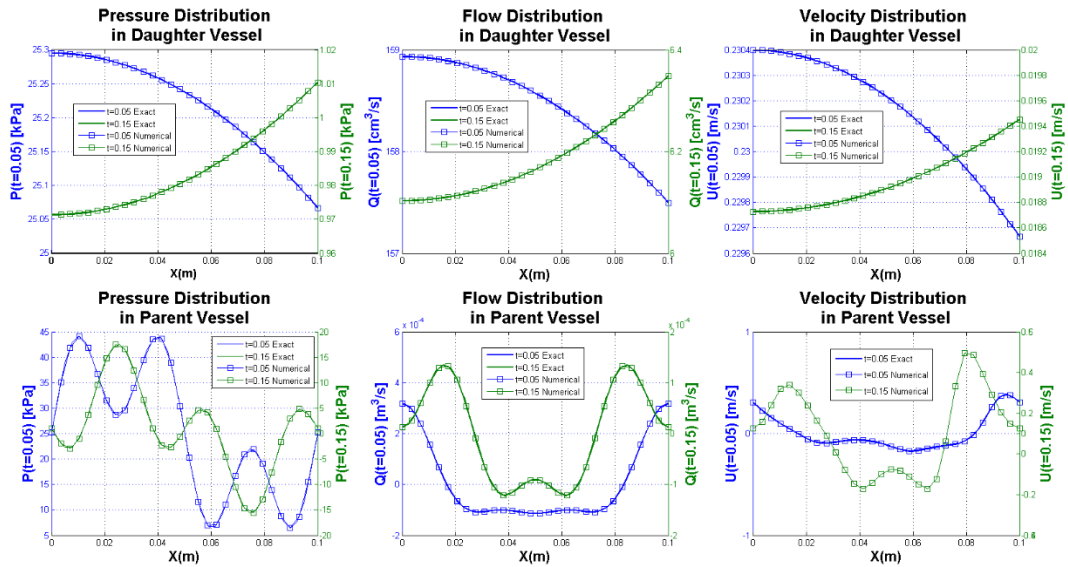


Fig. 5: FSI problem for bifurcated segments. Pressure, flow and velocity distributions in a parent and daughter vessels for $t=0.05s$ and $t=0.15s$. Numerical and manufactured solutions are not distinguishable.

4. Conclusions

A general approach to derive the fluid-structure interaction problem have been applied based on Hamilton's variational principle. Fluid is assumed viscous, and a boundary wall – nonlinear viscoelastic. Internal boundary conditions at the matching sections of a multiscale 3D-1D approach are derived. Numerical results based on a TVD approach compared to the solutions provided by the Lax-Wendroff. It is proved that the Lax-Wendroff method is clearly dispersive, providing artificially oscillations simulating physical problems with discontinuity. These oscillations are not present in TVD method, making it the optimum choice in solving 1D FSI problem. Derived internal boundary conditions enable the coupling of 1D FSI model to a local 3D FSI model of the arteries.

References

- [1] K. H. Parker, "A brief history of arterial wave mechanics," *Medical and Biological Engineering and Computing*, vol. 47, no. 2, pp. 111-118, 2009.
- [2] L. Formaggia, A. Quarteroni, A. Veneziani, Eds., *Cardiovascular Mathematics, of MS&A, — Modeling, Simulation and Applications*, vol. 1, Milan: Springer, 2009.
- [3] A. S. Liberson, J. S. Lillie, D. A. Borkholder, "A physics based approach to the pulse wave velocity prediction in compliant arterial segments," *Journal of Biomechanics*, 2016.
- [4] J. S. Lillie, A. S. Liberson, D. A. Borkholder, "Quantification of Hemodynamic Pulse Wave Velocity Based on a Thick Wall Multi-Layer Model for Blood Vessels," *Journal of Fluid Flow Heat and Mass Transfer*, vol. 3, pp. 54-61, 2016.
- [5] A. S. Liberson, J. S. Lillie, D. A. Borkholder, "Shock Capturing Numerical Solution for the Boussinesq Type Models with Application to Arterial Bifurcated Flow," *Proceedings of the International conference on New Trends in Transport Phenomena*, Canada, 2014.
- [6] V. Berdichevsky. *Variational Principles of Continuum Mechnaics*, 2010.
- [7] E. Kock, L. Olson. "Fluid-structure interaction analysis by the finite element method – a variational approach," *International Journal for Numerical Methods in Engineering*, vol. 31, pp. 463-491, 1991.
- [8] R. Leveque, *Finite Volume Methods for Hyperbolic Problems*. Cambridge: University Press, 2002.
- [9] Y. Kosolapov, A. Liberson, "An implicit relaxation method for computation of 3D flows of spontaneously condensing steam," *Computational Mathematics and Mathematical Physics*, vol. 37, no. 6, pp. 759-768, 1997.

- [10] A. Liberson, S. Hesler, T. Mc.Closkey, "Inviscid and viscous numerical simulation for non-equilibrium spontaneously condensing flows in steam turbine blade passages," *International Joint Power Generation Conference*, ASME, vol. 2, pp. 97-105, 1998.
- [11] Y. C. Fung, K. Fronck, P. Patitucci, "Pseudoelasticity of arteries and the choice of its mathematical expression," *Am J Physiol.*, vol. 237, no. 5, pp. H620-H631, 1979.
- [12] O. San, A. Staples, "An improved model for reduced order physiological fluid flows," *Journal of Mechanics in Medicine and Biology*, pp. 1-37, 2012.